BIOCHEMISTRY
including biophysical chemistry & molecular biology
Article

Biochemistry **2010,** *49,* 7255–7263 7255
DOI: 10.1021/bi100637n

Effect of the Protonation State of the Titratable Residues on the Inhibitor Affinity to BACE-1[†]

José L. Domínguez,[‡] Tony Christopeit,[§] M. Carmen Villaverde,[‡] Thomas Gossas,[§] José M. Otero,[‡] Susanne Nyström,[∥] Vera Baraznenok,[∥] Erik Lindström,[∥] U. Helena Danielson,*[,§] and Fredy Sussman*[,‡]

[‡]*Departamento de Química Orgánica, Facultad de Química, Universidad de Santiago de Compostela, 15782 Santiago de Compostela, Spain,* [§]*Department of Biochemistry and Organic Chemistry, Uppsala University, Uppsala, Sweden, and* [∥]*Medivir AB, Lunastigen 7, Huddinge, Sweden*

Received April 26, 2010; Revised Manuscript Received July 20, 2010

ABSTRACT: BACE-1 is one of the aspartic proteases involved in the cleavage of β amyloid peptide, an initial step in the formation of amyloid plaques whose toxicity induces neuron death in Alzheimer's disease patients. One of the central issues in the search of novel BACE-1 inhibitors is the optimum pH for the binding of inhibitors to the enzyme. It is known that the enzyme has optimal catalytic activity at acidic pH, while cell active inhibitors may bind optimally at higher pH. In this work we determine the effect of the pH on the affinities of a set of inhibitors, with a variety of chemical motifs, for the ectodomain region of BACE-1 by a surface plasmon resonance (SPR) biosensor based assay. In order to understand the molecular interactions that underlie the diverse optimum pH for the binding of the various inhibitors as observed experimentally, we have calculated the titration curves for a set of BACE-1 ligand complexes. The results indicate that the pK_a values of the titratable residues of the protein depend on the nature of the ligand involved, in disagreement with previous work. The enzyme−inhibitor structures with the resulting protonation states at pH values 4.5 and 7.4 served as the starting point for the prediction of the pH-dependent binding ranking. Our calculations reproduced the entire affinity ranking observed upon pH increase and most of the binding trends among inhibitors, especially at low pH. Finally, our cell-based assays indicate a possible correlation between high inhibitor affinity at both acidic and neutral pH values, with optimal cell response, a result that may open new venues for the search of potent BACE-1 inhibitors that are active at the cellular level.

Alzheimer's disease (AD)[1] is a widespread, neurodegenerative, dementia-inducing disorder which typically begins in middle to late adult life (*1*). It is characterized by synaptic loss and neuronal death in the cerebral cortex and the hippocampus. The major observed lesions are amyloid plaques, which are formed by the amyloid peptide (Aβ) fibril aggregates (*1*, *2*). The Aβ peptide, which contains 40−42 amino acids, is the product of a hydrolytic cleavage of the amyloid precursor protein (APP, a type I transmembrane glycoprotein), a process that is catalyzed by a tandem of two proteases identified as β- and γ-secretases (*2*−*7*). It has been demonstrated that the former enzyme (also referred to as BACE-1 and memapsin 2) participates in the rate-limiting step of the hydrolytic process that leads to the APP fragments, a fact that has converted β-secretase into a major target for drugs against Alzheimer's disease (*3*−*7*). As a result, many pharmaceutical companies and academic institutions became involved in drug discovery efforts targeting this enzyme (*2*, *8*).

The main aim of these efforts is the discovery of small molecular weight compounds that can trespass the blood brain barrier. Many first generation peptidomimetic inhibitors with low nanomolar affinities in enzyme-based assays are not active in cell-based assays because of the limited penetration across cell membranes (*9*). Higher bioavailability may be precluded (in part) by the large number of polar groups present in peptidic inhibitors. In principle, the automated screening of compounds belonging to chemical libraries or resulting from combinatorial chemistry could provide nonpeptidic inhibitors with the right balance of polar and nonpolar groups. Nevertheless, the earliest high-throughput screening (HTS) of putative β-secretase inhibitors did not prove to be very successful. For instance, Coburn et al. reported that a single molecule (a 1,3,5-trisubstituted benzene) emerged as a hit from a HTS of a multimillion compound library (*10*). Other approaches to inhibitor design have relied on small fragment-based screening (FBS) by X-ray and NMR techniques (*11*). These protocols have led to the discovery of chemically diverse nonpeptidic inhibitors that in some cases have a novel binding mode that displays a more open active site of the enzyme (*12*).

[†]This work was supported by financial aid from the Ministerio de Educación y Ciencia (MEC), Spain, and the Xunta of Galicia to M.C.V. and F.S., the Carl Tryggers Stiftelse för Vetenskaplig Forskning, Sweden, to U.H.D., and scholarships to J.L.D. from the MEC and to T.C. from the Sven and Lilly Lawski Fund. The Supercomputing Center of Galicia (CESGA) provided computer time.

*To whom correspondence should be addressed. (F.S.) Phone: 34-881-814402. Fax: 34-981-595012. E-mail: fredy.sussman@usc.es. (U.H.D.) Phone: +46 18 4714545. Fax: + 46 18 558431. E-mail: helena.danielson@biorg.uu.se.

[1]Abbreviations: AD, Alzheimer's disease; BACE-1, β-site APP cleaving enzyme; APP, amyloid precursor protein; SPR, surface plasmon resonance; FBS, fragment-based screening; EM, energy minimization; NOE, nuclear Overhauser effect; MD, molecular dynamics; CHARMM, chemistry at Harvard molecular mechanics; ABNR, adopted basis set Newton−Raphson; NVT, MD protocol where the number of molecules, the volume, and the temperature are kept constant; GBSW, generalized Born with simple switching; DS, discovery studio; HTS, high-throughput screening; FRET, fluorescence resonance energy transfer; HE, hydroxethylene; HEA, hydroxylethylamine; RU, resonance units.

Published on Web 07/26/2010

There are several issues related to the computer-aided design of novel ligands that could enhance the success of HTS and FBS protocols but that have not been fully addressed yet. One of the most vital ones is the protonation state of the many buried acidic residues found in this protein, including the active site Asp dyad, which lends to this enzyme an optimal catalytic activity at low pH (*3*). Most of the inhibitors developed at the earliest stages were transition state analogues with various degrees of peptidic nature and probably have their highest affinity at the pH value optimal (4.5) for activity (*2*, *13*). But many subsequent inhibitor design cycles, like the one based on small fragment search by X-ray crystallography, have generated compounds that anchor themselves to the Asp dyad by amine groups (*12*), and it is not clear what their effect on the protonation state of buried acidic residues like the ones that belong to the Asp dyad will be. There have been many attempts to search for putative inhibitors by an *in silico* HTS screening, but they have always relied on a single BACE-1 Asp dyad protonation state, in spite of the large chemical diversity found in the chemical libraries used in HTS. Nevertheless, some authors claim that a given Asp dyad protonation state results in an enrichment of high-affinity molecules in the final set, when used instead of alternative protonation states (*14*, *15*).

There have been many attempts to predict the charged state of the active site Asp dyad by computational methods that include molecular mechanics (*16*), quantum mechanical calculations (*17*), or a combination of both protocols (*18*). The calculations were performed on a single complex formed by BACE-1 bound to inhibitor **OM99-2**. The results of those calculations support the hypothesis that the most favored Asp dyad charge state is the one that has only one of the Asp residues protonated. There has been only one attempt to calculate the pH dependence on the active site protonation state (*15*).

BACE-1 inhibitors bind to this enzyme in cellular compartments that probably display a neutral pH. Nevertheless, BACE-1 is most active at an acidic pH (4.5−5.5). To bridge this disconnect, we have studied the binding affinity of a set of chemically diverse inhibitors by surface plasmon resonance (SPR) biosensor technology at the pH of optimal activity for BACE (i.e., 4.5) and at a pH close to a neutral value that has been used in the X-ray studies of many BACE-1/inhibitor complexes (i.e., 7.4).

In order to understand the SPR biosensor observed pH dependence on ligand binding, we have calculated the titration curves for the enzyme−inhibitor complexes studied experimentally by an approximate solution of the Poisson−Boltzmann equation that employs a generalized Born approximation (*19*). These simulations afforded the protonation states of all titratable residues at both (4.5 and 7.4) pH values and allowed us to calculate the pH dependence of the binding affinities for those complexes. The calculated binding ranking pH dependence reproduces quite well the observed experimental trends for single inhibitors. Moreover, the underlying predicted protonation states indicate that the actual catalytic Asp dyad protonation state will depend strongly on the chemical structure of the inhibitor, in contrast to the consensus that has been arrived at in the literature. Our calculations explain the seemingly incongruous binding affinity pH dependence, providing a clear rationale based on the protonation states of the acidic residues (especially the Asp dyad), elicited by the chemically diverse inhibitors studied here.

Finally, our cell-based assays indicate that those inhibitors that display a high binding affinity at both acidic and neutral pH values present the best biological activity at the cell level, a result that opens new venues for the search of potent BACE-1 inhibitors that are effective at the cellular level.

MATERIALS AND METHODS

(*1*) *SPR Biosensor Interaction Analysis and Cellular Activity Studies*. (*a*) *Inhibitors*. The chemical structures of the inhibitors as well as the PDB codes of the complexes studied here are shown in Table 1. Inhibitors **I-2** (*20*), **I-3** (*21*), **I-4** (*22*), **I-5** (*23*), and **I-6** (*24*) were synthesized according to published procedures, while compound **I-1** (**OM99-2**) was obtained from Sigma-Aldrich, St. Louis, MO.

(*b*) *Protein*. The ectodomain of BACE-1 (amino acids 42−446) was expressed in *Escherichia coli* and purified to homogeneity according to previously published procedures (*25*).

(*c*) *Preparation of Biosensor Surfaces*. All interaction studies were performed at 25 °C with a Biacore 2000 or a Biacore S51 instrument (GE Healthcare, Uppsala, Sweden). The interaction was measured in resonance units (RU) as a function of time, and presented graphically as sensorgrams, with data from a series of inhibitor concentrations overlaid for each experiment. Prior to immobilization of BACE-1, the buffer of the purified enzyme was changed to 10 mM sodium acetate, pH 4.5, and the concentration adjusted to 0.1 mg/mL. The protein was immobilized to CM5 sensor chips by amine coupling according to standard procedures (GE Healthcare, Uppsala, Sweden). The running buffer during immobilization was 0.01 M Hepes, pH 7.4, and 0.15 M NaCl. A reference flow cell was prepared by activation and deactivation of the sensor surface.

(*d*) *Inhibitor Interaction Studies*. The interaction studies for all inhibitors were performed at a flow rate of 30 μL/min and in a running buffer composed of 10 mM Hepes, pH 7.4, 0.15 M NaCl, and 3% DMSO or 10 mM sodium acetate, pH 4.5, 0.15 M NaCl, and 3% DMSO. The inhibitors were diluted in running buffer and injected in two independent concentration series for 180 s. The dissociation was recorded until the inhibitor had cleared the surface, but at least for 600 s. A blank, consisting of running buffer, was injected before and after each concentration series.

BIAevalution 4.1 software (GE Healthcare Biosciences, Uppsala, Sweden) was used to analyze the data. The reference and an average of the blanks were subtracted from the data before determining the kinetic parameters using global nonlinear regression analysis and a 1:1 binding model with mass transfer. In order to compensate for bulk changes between the association and dissociation phase, an additional term for correction was included in the analysis model. The sensorgrams were normalized to the immobilized protein amount and the molecular weight of the compound.

(*e*) *Cellular Enzyme Activity Assay*. HEK293 cells stably expressing Swedish mutant APP (*26*) were cultured in DMEM supplemented with 10% FCS, PEST (50 units of penicillin/50 μg/mL streptomycin), and 200 μg/mL hygromycin at 37 °C and 5% CO_2. Cells of 2×10^4 per well were seeded into 96-well plates and left overnight to settle. Cells were washed with fresh media, and inhibitor was added at various concentrations in DMEM medium supplemented with FCS (10%) and hygromycin (200 μg/mL). The maximal DMSO concentration was kept below 1%. After 24 h, the cell culture media was harvested, and the amount of Aβ peptide was determined by Aβ x-40 ELISA (The Genetics Co.,

Table 1: Chemical Structures of the BACE-1 Inhibitors Studied

PDB code	Name	Structure
1FKN	OM99-2 (I-1)	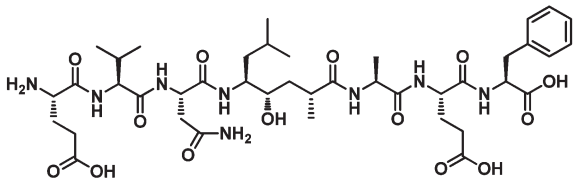
1M4H	OM00-3 (I-2)	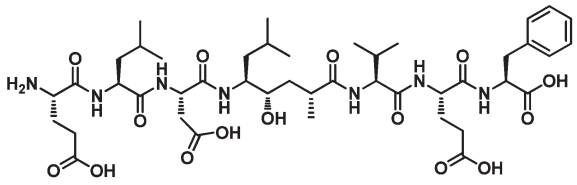
2B8L	I-3	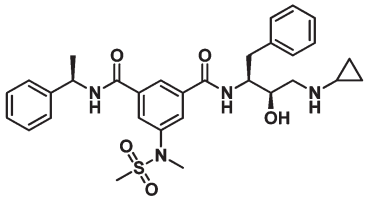
2IRZ	I-4	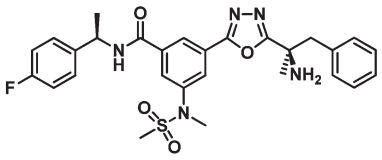
2VNN[a]	I-5	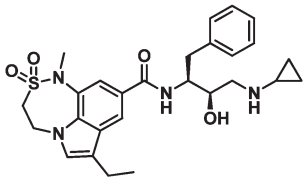
2VKM	I-6	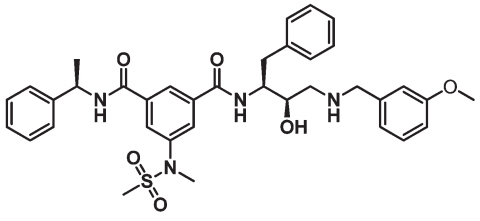

[a]The BACE-1−inhibitor complex for **I-5** was generated by homology with the **2VNN** complex.

Schlieren, Switzerland) according to instructions supplied by the manufacturer. The IC_{50} values were calculated from concentration−response curves using the Hill equation and GraphPad Prism software (San Diego, CA).

(*2*) *Simulation Protocols for pK_a and Binding Affinity Prediction*. (*a*) *Structure Preparation*. The structures studied in this work (see Table 1) were downloaded from the Protein Data Bank, and hydrogens were added using the Discovery Studio (DS) suite of programs (*27*). We excluded compound **I-6** from our simulation studies, since its slow dissociation rate as measured by SPR experiments only afforded a upper limit for its K_D value (K_D < 10 nM). Some of the structures have a segment missing between residues 158 and 169 (**2B8L**, **2IRZ**) or between residues 157 and 167 (**2VNN**). The missing loop was modeled in these complexes based on the template provided by the crystallographic structure of **1FKN**. Inspection of the incomplete structures indicated that the segments before the missing loop were frayed, making the insertion of the loop difficult. To avoid this problem, we adjusted the torsional angles of the unraveled residues to their values observed in the **1FKN** complex. Once this was achieved, the loop was put into place by attaching its N- and C-terminals to the protein. To optimize this segment of the structure, we performed an energy minimization (EM) on a protein segment that included the inserted strain and five residues to either side of the above-mentioned fragment. For this sake we used a steepest descent protocol with a 0.1 kcal/(mol Å^2) gradient tolerance, using a CHARMM force field (*28*) available in the Discovery Studio suite of programs (*27*). Since

the coordinates of the complex BACE-1/**I-5** have not been published, we have generated them from the **2VNN** complex by replacing the *m*-(trifluoromethyl)benzyl moiety in this complex (*23*) by a cyclopropane fragment, using as a template the conformation of inhibitor **I-3**, which also has the same fragment at its C-terminal end.

(*b*) *pK_a and Binding Affinity Prediction*. The pK_a values for all titrable residues at a range of pH values (2−12) were calculated by the protocol proposed by Spassov and Yan (*19*), implemented in Discovery Studio and named Calculation of Protein Ionization and Residue pK_a. This protocol, which employs a generalized Born approximation to reproduce solvent effects, allows for the iterative determination of the pK_a of interacting residues. The internal and external dielectric constants used in these calculations were 10 and 80, the ionic strength was 0.145, and the energy cutoff for clustering was 0.5 kcal/mol. The charges used in these calculations were obtained from the CHARMM force field (*28*). The protocol used here for the prediction of the pK_a value of ionizable residues (see Spassov and Yan (*19*)) applies to all residues of the protein and to the amino acids that form part of the inhibitor. Hence, this algorithm was able to predict the pK_a values (and hence the protonation fraction at a given pH) for the acidic amino acids in inhibitors **I-1** and **I-2** and the ionizable groups at their N- and C-terminal ends. The amino groups of inhibitors **I-3 to I-5** may have a pK_a value as high as 10 or 11, and hence we have left them charged.

These calculations produce titration curves that depict the degree of protonation of each ionogenic residue at every pH value. The DS module also generates the preponderant protonation state at a given pH value, placing a proton on all residues that have a protonation fraction above 0.5. In some BACE-1−inhibitor complexes it was found that some residues (i.e., Asp228) have a protonation fraction just below 0.5. In this case, the alternative protonation state (i.e., protonated Asp228) was also generated and used for affinity calculations (see below).

For our binding affinity calculations we chose the protonation states predicted as the prevalent ones at pH 4.5 and 7.4 on the basis of the calculated protonation fraction for each residue by the pK_a predictor DS module. The resulting structures were subjected to a multistep molecular mechanics optimization protocol. The first part incorporated two energy minimization protocols devoted to optimize the proton position and the hydrogen bond ligand−protein network observed in the crystallographic structure. In the first EM we fixed all heavy atoms, while in the second we placed NOE constraints on the heavy atoms that participate as donors and acceptors in hydrogen bonds between the ligand and the protein. Each of the EM had two segments: the first one was an EM steepest descent segment of 2000 steps, and the second one was a stage of 50000 steps with an ABNR optimization protocol. The tolerance gradient in all of these calculations was 0.001 kcal/(mol Å^2). The resulting structure was subjected to a NVT molecular dynamics (MD) protocol close to 0.5 ns in length, consisting of 6 ps of heating, 60 ps of equilibration, and 400 ps of production at 300 K. For all of the EM and MD calculations we used an implicit solvation term based on the generalized Born approach with simple switching (GBSW) (*29*). In the MD production stage molecular conformations were collected every 2 ps for subsequent ligand−protein analysis by a scoring function built upon the difference in energy between the enzyme−inhibitor complex and its components and averaged over a set of MD generated conformations. Hence the binding affinity scoring function can be written as

$$\langle \Delta G_{\text{bind}} \rangle = \langle \Delta G_{\text{mm}}(\text{P:L}) - \Delta G_{\text{mm}}(\text{P}) - \Delta G_{\text{mm}}(\text{L}) + \Delta G_{\text{gb}}(\text{P:L}) - \Delta G_{\text{gb}}(\text{P}) - \Delta G_{\text{gb}}(\text{L}) \rangle \quad (1)$$

where ΔG_{mm} and ΔG_{gb} indicate the molecular mechanics CHARMM force field (*28*) and the GBSW solvation (*29*) components, respectively, for the protein−ligand complex (P:L), protein (P), and ligand (L).

All of the EM, MD, and analysis calculations were performed with the CHARMM suite of programs (*30*) in the 2400 processor Finisterrae supercomputer facility available at the Supercomputing center of Galicia (CESGA).

RESULTS AND DISCUSSION

(*1*) *Interaction Analysis*. The interaction of the BACE-1 inhibitors selected for this study (Table 1) with BACE-1 was analyzed at pH 4.5 and 7.4 (Figure 1). There were significant differences in the interactions for the different compounds and the two conditions. Compounds **I-3** to **I-5** interacted reversibly with the enzyme at both pH values (Figure 1). The affinities could be estimated (Table 2) by globally fitting a 1:1 interaction model with mass transfer limitation to the complete association and dissociation phase data. Due to the slow dissociation rates, the kinetics or affinities could not be determined for **I-1** and **I-2** at pH 4.5 and for **I-6** at both pH values. K_D values were defined to be below 10 nM for the sake of the quantitative analysis. The slow dissociation should be borne in mind when interpreting enzyme inhibition data for these compounds as steady-state inhibition experiments assume that the interaction is reversible, which clearly may not be the case.

(*2*) *Titration Behavior of Ionogenic Residues*. (*a*) *Active Site Asp Dyad Protonation State*. Figure 2 shows the calculated titration curves for the Asp dyad residues for the complexes studied here. It depicts the protonation fraction (*X*), the amount of each of the Asp dyad side chain residues that is protonated, as a function of the pH value. The most common feature in this figure is that the residue Asp32 stays protonated at a larger range of pH values than its Asp dyad partner, Asp228. Nevertheless, the chemical structure of the inhibitor seems to have a very strong influence on the actual shape of the titration curves and specifically on the protonation fraction at the pH values we are most interested in (i.e., 4.5 and 7.4). For instance, when BACE-1 is bound to peptidic inhibitors with a hydroxyethylene (HE) group in their isostere (**1FKN**, **1M4H**) (*13*, *20*), both Asp dyad partners remain protonated until or beyond pH 6, due to their large pK_a shift from their solution value (around 3.9), leading to a doubly protonated state at pH 4.5 and mainly a monoprotonated state at pH 7.4 for the Asp dyad. On the other hand, our calculations predict that the presence of an amino group that interacts with one or both members of the Asp dyad (**2B8L** (*21*), **2VNN** analogue (*23*), or **2IRZ** (*22*)) reduces their pK_a to values closer to the ones in solution (especially for the case of Asp228). The difference between the HE-based inhibitors and the latter type of ligands may reside in the fact that the ammonium group has a high pK_a value (ca. 10) and will remain charged inside the protein, providing a polar environment that helps to lower the Asp residue pK_a values. For this reason, the inhibitors containing hydroxylethylamine (HEA) or those containing an amino group

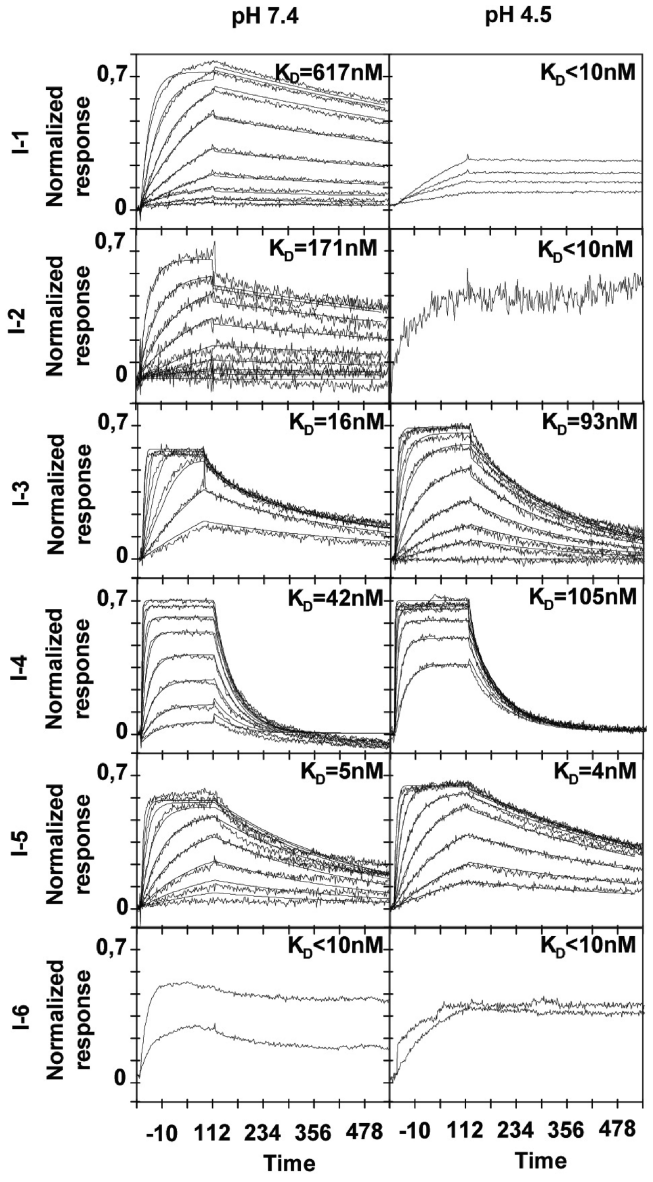

FIGURE 1: Interaction data for inhibitors **I-1** to **I-6** with BACE-1. The sensorgrams were normalized to the theoretical maximum signal estimated from the mass of the inhibitor and the amount of immobilized protein. A 1:1 binding model with mass transfer was fitted to the complete association and dissociation data, shown as solid lines, and the corresponding K_D values are given. For interactions where the affinities could not be estimated, an upper limit is given.

promote a monoprotonated dyad at a low pH value. At a higher pH value (7.4) this effect leads to an Asp dyad monoprotonated state (**2B8L**, **2VNN** analogue) or to a fully doubly charged Asp dyad as in the case of the complex **2IRZ**.

Our calculations are at variance with the consensus that was built by inference from experiments on other aspartic proteases (HIV-1 PR (*31*, *32*), endothiapepsin (*33*), etc.) and from the calculations performed on the BACE/**OM99-2** complex (*16*−*18*). The computer-assisted studies of the dyad protonation state reached a consensus that the Asp dyad is monoprotonated, but they disagree on which Asp residue the proton resides (*2*). The earliest attempt to assign a charge to the catalytic dyad was based on molecular dynamics (MD) simulations of the X-ray structure of the β-secretase complexed with **OM99-2** in solution (*16*). The starting points for the MD simulations assumed a charge of −1 for the Asp dyad but differed on the charge assignment, with either the Asp32 or the Asp228 ionized. Their results indicate that a neutral Asp32 and ionized Asp228 combination is the only option that maintains the intricate network of hydrogen bonds around the Asp dyad observed in the X-ray structure (*16*). This outcome is in agreement with our results for the **1FKN** complex at high pH value, the one used for the determining its structure by X-ray crystallography. Nevertheless, as pointed out above, our calculations suggest that the dyad is totally neutralized at the pH at which the enzyme presents its highest activity (pH 4.5). Other calculations carried out on the **1FKN** complex, like the linear scaling quantum approach, supported a monoprotonated state Asp dyad with a neutralized Asp228 and a charged Asp32 (*17*), in contrast to the conclusions based on the titration curves presented here.

(*b*) *Total Formal Charge as a Function of pH*. Most previous calculations aimed at studying the active site protonation state of BACE-1 have not taken into account the effect of the pH (*16*−*18*). Furthermore, the aim of the only pH-related study was to elucidate the Asp dyad protonation state and to apply it to an *in silico* screening of a large number of compounds with high chemical diversity (*15*). As far as we can judge, no effort has been made to study the protonation state of other ionizable residues. For most proteins that would not be a problem since most of the charged residues will be accessible to solvent and hence would remain charged for all pH values of interest. The aspartic protease family (to whom BACE-1 belongs) represents an exception in this regard, since they have a substantial number of titrable acidic residues that are partially or totally buried inside the protein. For this reason their pK_a values could be substantially larger than those of model compounds in solution, an effect that would depend on the polarity of the microenvironment where they are buried. Figure 3 graphically shows the BACE-1 charged states of the titrable residues. Perusal of this figure indicates that a number of acidic residues get ionized as the pH value increases. We have partly quantified this effect in Table 3, which lists the calculated pK_a values of the BACE-1 buried acidic residues. The results shown in this table indicate that the biggest shift in pK_a with respect to their values in solution is experienced by the residues of the active site Asp dyad. Interestingly enough, some of the buried acidic amino acids that experience a rise in their pK_a values are Glu residues, while some of the Asp residues reduce their pK_a value. Scrutiny of the **1FKN** structure indicates that some of the buried amino acids manage to keep low pK_a values (shown in Table 3) because they reside in a buried polar microenvironment, where sometimes they can form ion pairs with basic residues. Many of the residues listed in Table 3 have a pK_a value between 4.5 and 7.4 and hence will undergo a change in protonation state upon a pH increase, a result that will translate into changes in the catalytic efficiency as well as ligand affinity, the issue that will be discussed below.

(*3*) *Evaluating Binding Affinities at Different pH Values*. The starting point for the evaluation of the effect of the pH on ligand binding affinities was the structure of the BACE-1−ligand complexes in which the ionogenic residues are in their prevalent protonation states (as predicted by their calculated degree of protonation). In some systems the degree of protonation of the acidic residues, such as Asp228 (a member of the Asp dyad), is only slightly lower than 0.5, as in the case of the **2B8L** complex. Hence, our calculations predict nonnegligible populations in the neutral charge state for residues such as Asp228. In order to estimate the effect of the "minority" Asp dyad protonation state, we evaluated the ranking by using our scoring function (see eq 1

Table 2: Cell Assay Data and pH Effect on Experimental and Calculated Affinity Values

			K_D (nM)[c]		scoring function (kcal/mol)[d]	
PDB code	inhibitor	cellular IC_{50} (nM)[b]	pH 4.5	pH 7.4	pH 4.5	pH 7.4
1FKN	**OM99-2 (I-1)**	940	< 10	617 ± 2.8	−65.0 ± 3.4	−57.2 ± 3.1 (−55.0 ± 3.3)
1M4H	**OM00-3 (I-2)**		< 10	171 ± 19	−71.4 ± 2.8	−53.0 ± 3.4 (−53.1 ± 3.3)
2B8L	**I-3**	22	93 ± 17	16 ± 3	−59.8 ± 3.3 (−58.4 ± 3.3)	−61.0 ± 3.0
2IRZ	**I-4**	86	105 ± 34	42 ± 20	−45.8 ± 3.8	−53.2 ± 2.4
2VNN[a]	**I-5**	3	4 ± 0.3	5 ± 0.8	−45.2 ± 3.6	−45.5 ± 3.9
2VKM	**I-6**	0.1	< 10	< 10		

[a]**2VNN** analogue. [b]Inhibition of Aβ production in HEK293 cells stably transfected with Swedish mutant APP. [c]The standard deviations are based on at least two independent experiments. [d]Values in parentheses were calculated by weighting the affinities with their protonation fraction states when those values are close to 0.5.

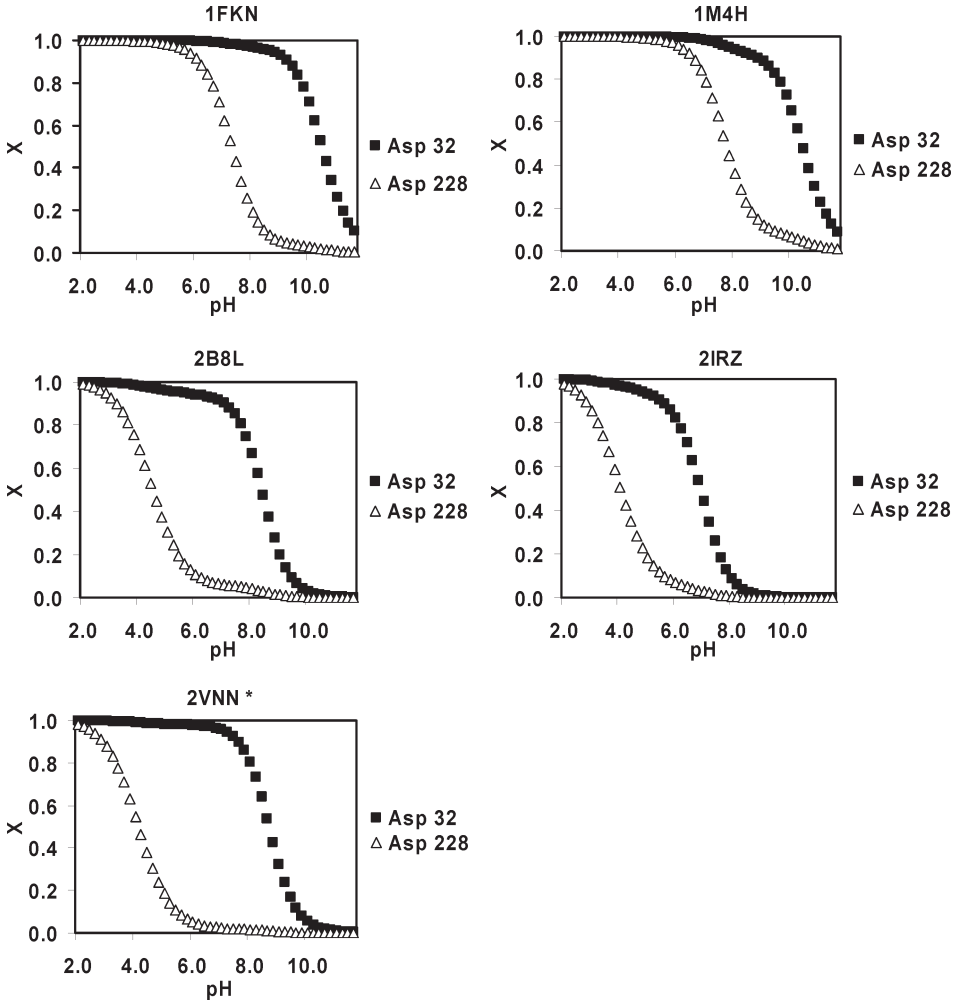

FIGURE 2: Titration curves for the active site Asp dyad in BACE-1. The titration curves show the fraction protonated (X) as a function of pH for Asp32 (black squares) and Asp228 (white triangles) in the BACE-1−inhibitor complexes studied in this work.

in Materials and Methods section) with the alternative Asp228 protonation state as well. The final inhibitor affinity prediction was obtained by weighting the calculated scoring function of the BACE-1−ligand complexes in both protonation states by each of the protonation fractions calculated at the relevant pH value. Table 2 displays the dissociation constants (K_D) obtained by SPR biosensor experiments, together with the results of the affinity scoring at both pH values calculated from eq 1. The energy values in this table were the result of an average over the 100 conformations with the lowest scoring function values. Including all conformations from the MD production trajectory did not change any of the binding trends calculated as indicated before (results not shown). Values in parentheses refer to the weighted scoring function, when the fraction of the protonated state for this residue is very close to 0.5.

Table 2 enables us to compare the calculated binding ranking of the inhibitors with the experimental one. As seen from this table, our scoring function reproduces the ranking of binding for every inhibitor upon a pH increase. For instance, our calculations show that the ligands that contain an isostere with a

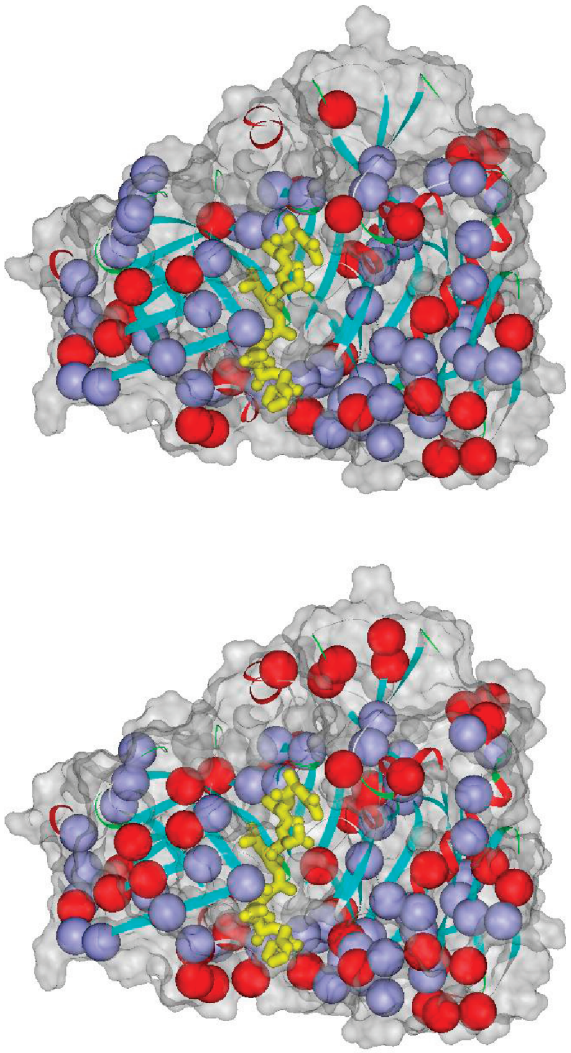

FIGURE 3: Charged residues as a function of pH value calculated for the **1FKN** complex. The upper panel corresponds to pH 4.5 and the lower panel to pH 7.4. Acidic residues are depicted as red and basic residues as blue spheres. The inhibitor is drawn in yellow sticks. The complex is represented by its water-accessible surface (shown in gray).

Table 3: pK_a Values for Buried Residues

	PDB code				
residue[a]	**1FKN**	**1M4H**	**2B8L**	**2IRZ**	**2VNN**[b]
Asp 32	10.46	10.35	8.35	6.88	8.67
Asp 83	4.49	4.74	4.79	4.87	4.83
Asp 138	2.98	3.11	3.23	3.38	3.41
Asp 228	7.26	7.68	4.47	4.01	4.11
Asp 311	3.04	3.53	3.88	3.59	3.62
Asp 346	4.46	4.46	4.55	4.59	4.49
Asp 363	3.34	3.25	3.08	3.06	3.24
Glu 116	5.66	6.07	5.95	6.09	5.80
Glu 200	5.95	5.63	5.50	5.52	5.43
Glu 207	4.79	4.67	5.02	5.02	4.60
Glu 219	4.40	4.38	4.06	4.61	4.57
Glu 339	6.72	6.73	6.10	6.26	6.44

[a]The pK_a values for Asp and Glu residues in solution are 3.9 and 4.2, respectively. [b]**2VNN** analogue.

hydroethylene motif are predicted to have their highest affinity for the protein at the pH value at which the enzyme has the highest catalytic activity (4.5), in agreement with the observed affinities. This trend stands to reason since the isosteres in these inhibitors (**OM99-2** and **OM00-3**) are transition state analogues and their ligand binding affinity ranking upon pH change should mimic that of the pH dependence of substrate binding (*34*). When the anchoring motif to the Asp dyad is an amino group, this trend inverts, and the highest affinity is observed at pH 7.4, also in agreement with experiment. The rationale behind this behavior could be possibly found in the charged nature of the amino group. As pointed out above (see section 2a), this group has a pK_a value around 10 in solution and would likely remain protonated inside the protein and induce the ionization of the Asp dyad, resulting in the formation of a salt bridge between both charged groups and hence raising the affinity of the ligand for the protein at this pH value. The K_D values obtained from SPR biosensor experiments indicate that those inhibitors with a mixed isostere's anchoring motif (i.e., those with a hydroxylethylamine motif) have a mixed behavior regarding the optimal pH for inhibitor binding to the protein, a trend that is predicted by our scoring function calculations as well. As can be seen from Table 2 compound **I-5** shows almost equal K_D at both pH values, while compound **I-3** has a higher affinity for the enzyme at higher pH. In the case of the **2B8L** complex, the resulting binding affinity pH dependence could be traced back at least in part to the Asp dyad possible multiple protonation state. While the Asp32 has a predicted pK_a value of 8.4 and hence will remain protonated at both pH values, the other member of the Asp dyad (Asp228) has a pK_a value only slightly lower than 4.5 (see Table 3), which will result in an almost equal population of charged and uncharged species at the lower pH. In this case we have performed a weighted binding affinity prediction as described in our Materials and Methods section. As seen from Table 2, the results agree slightly better with the K_D trend, when we average the binding affinities for the enzyme in both Asp228 protonation states, using as weights the fraction of protonation state of the Asp228 in both protonated states.

Furthermore, the affinity rankings for all of these inhibitors (with the exception of **I-5**) are well reproduced at low pH by our scoring function, in spite of its simplicity and absence of any adjustable parameters. For instance, our scoring function predicts that the transition state analogue inhibitors (e.g., **OM99-2** and **OM00-3**) are more potent than the HEA or amino-containing inhibitors at low pH, in agreement with the experimental K_D values. Although the slow dissociation of compounds **I-1** and **I-2** prevented the affinities to be estimated by the biosensor-based interaction experiments, FRET-based inhibition assays using the ectodomain region of BACE-1 indicate that the latter inhibitor is more potent than the former (data not shown), in agreement with our scoring function predictions (*20*). Our scoring function does not reproduce the experimental affinity trends as well amongst inhibitors at the higher pH values or across pH values.

(*4*) *Correlation between Binding Affinities at Acidic and Neutral pH with Cell Activity*. Since aspartic proteases generally present their highest activity at acidic pH values, it is believed that they act in cell compartments where the pH is low. Nevertheless, BACE-1 is found at the cell surface where pH is neutral. Furthermore, it was found recently that some BACE-1 inhibitors based on aminoheterocyclic fragments have a cell readout activity in the low micromolar range and an enzyme affinity in the same range at pH close to neutral (6.5) (*35*). As seen

from Table 2, the cell assays performed in our laboratory indicate that those inhibitors that have a high enzyme affinity at both high and low pH values (i.e., those inhibitors with a HEA moiety) also show high activity at the cellular level. A possible explanation for these results is that although BACE-1 is catalytically active once transported to endosomal vesicles where the pH is acidic, only compounds that also interact with the enzyme at neutral pH will be cotransported with the enzyme into this compartment. Hence, compounds that bind BACE-1 well at acidic as well as neutral pH values could in principle be good candidates for optimal performance at the cellular level, a design avenue for cell active compounds which we are going to explore for a larger number of compounds. The results presented here indicate that our computer-assisted protocols for the evaluation of the pH dependence could be ideally suited to assist in the design of cell active analogues.

In conclusion, we have studied the effect of pH on the binding affinities of a group of BACE inhibitors with a variety of chemical motifs by SPR. The seemingly incongruous experimental pH effect on the binding affinities was explained with the help of molecular mechanics-based calculations. The synergy between both approaches provides a number of interesting insights into the molecular recognition processes at a molecular level that underlie the observed binding affinities at different pH values. To the best of our knowledge the important issue of the dependence of ligand affinity on the ionization states of the protein residues and the ligand has only been sparingly addressed in the literature (*36*).

Our calculations reproduce the entire observed affinity ranking upon pH increase and most of the binding trends among inhibitors at low pH values. The agreement between the observed and calculated binding ranking lends support for the pK_a assignments afforded by the simple protocol used here, indicating that pK_a calculations by an approximation to the Poisson−Boltzmann approach have come a long way (*19*) and their outcome may rival that of more sophisticated protocols.

The binding pH dependence could be traced back to the protonation state of the titratable residues in the pH range studied. The results indicate that the pK_a values of the protein titratable residues, especially those that are close to the inhibitor, depend strongly on the nature of the ligand involved, in disagreement with earlier work (*14*, *15*). Perusal of the predicted Asp dyad protonation states underscores the pK_a dependence on the inhibitor's chemical nature. Our calculations indicate that inhibitors with the HE isostere motif (i.e., **OM99-2** and **OM00-3**) induce a diprotonated state at low pH (4.5), while the probability of a monoprotonated Asp dyad increases at higher pH (i.e., 7.4). Other isosteres, which include an amino group as its binding motif to the Asp dyad, lower the Asp dyad pK_a values (see Figure 2 and Table 3), generating monoprotonated and fully ionized Asp dyad states at both pH values. In a few cases, the Asp dyad can be populated by two alternative protonation states that could be taken into account in order to get a result that is more in line with the observed binding affinities.

Our results suggest that it might not be advisible to perform an *in silico* HTS search of fragments or BACE-1 putative ligands with one single protonation state across the board, as done previously by several research groups (*14*, *15*). More likely, the ligands would have to be classified in accordance with the protonation state they can elicit from the Asp dyad, and then the HTS screening could proceed with several enzyme targets differing in their protonation states.

As pointed out above, the pH values of the medium surrounding BACE-1 vary with the cell compartments where the enzyme is located. Nevertheless, we have shown in this work that the inhibitor activity at cell level may be related to high inhibitory potency at both acidic and neutral pH values. Computer-aided design based on the protocols introduced in this work could be very valuable in the search of inhibitors that exhibit this trait.

ACKNOWLEDGMENT

We thank Dr. Eva Muñoz for helpful discussions.

REFERENCES

1. Selkoe, D. J. (1999) Translating cell biology into therapeutic advances in Alzheimer's disease. *Nature 399*, A23–A31.
2. Villaverde, M. C., González-Louro, L., and Sussman, F. (2007) The search for drug leads targeted to the β-secretase: an example of the roles of computer assisted approaches in drug discovery. *Curr. Top. Med. Chem. 7*, 980–990.
3. Lin, X., Koelsch, G., Wu, S., Downs, D., Dashti, A., and Tang, J. (2000) Human aspartic protease mepapsin 2 cleaves the β-secretase site of β-amyloid precursor protein. *Proc. Natl. Acad. Sci. U.S.A. 97*, 1456–1460.
4. Vassar, R., Bennett, B. D., Babu-Khan, S., Khan, S., Mendiaz, E. A., Denis, P., Teplow, D. B., Ross, S., Amarante, P., Loeloff, R., Luo, Y., Fisher, S., Fuller, J., Edenson, S., Lile, J., Jarosinski, M. A., Biere, A. L., Curran, E., Burgess, T., Louis, J.-C., Collins, F., Treanor, J., Rogers, G., and Citron, M. (1999) β-Secretase cleavage of Alzheimer's amyloid precursor protein by the transmembrane aspartic protease BACE. *Science 286*, 735–741.
5. Yan, R., Bienkowski, M. J., Shuck, M. E., Miao, H., Tory, M. C., Pauley, A. M., Brashler, J. R., Stratman, N. C., Mathews, W. R., Buhl, A. E., Carter, D. B., Tomasselli, A. G., Parodi, L. A., Heinrikson, R. L., and Gurney, M. E. (1999) Membrane-anchored aspartyl protease with Alzheimer's disease β-secretase activity. *Nature 402*, 533–537.
6. Sinha, S., Anderson, J. P., Barbour, R., Basi, G. S., Caccavello, R., Davis, D., Doan, M., Dovey, H. F., Frigon, N., Hong, J., Jacobson-Croak, K., Jewett, N., Keim, P., Knops, J., Lieberburg, I., Power, M., Tan, H., Tatsuno, G., Tung, J., Schenk, D., Seubert, P., Suomensaari, S. M., Wang, S., Walker, D., Zhao, J., McConlogue, L., and John, V. (1999) Purification and cloning of amyloid precursor protein β-secretase from human brain. *Nature 402*, 537–540.
7. Hussain, I., Powell, D., Howlett, D. R., Tew, D. G., Meek, T. D., Chapman, C., Gloger, I. S., Murphy, K. E., Southan, C. D., Ryan, D. M., Smith, T. S., Simmons, D. L., Walsh, F. S., Dingwall, C., and Christie, G. (1999) Identification of a novel aspartic protease (Asp 2) as β-secretase. *Mol. Cell Neurosci. 14*, 419–427.
8. Ghosh, A. K. (2009) Harnessing nature's insight: design of aspartyl protease inhibitors from treatment of drug-resistant HIV to Alzheimer's disease. *J. Med. Chem. 52*, 2163–2176.
9. Hanessian, S., Yun, H., Hou, Y., Yang, G., Bayrakdarian, M., Therrien, E., Moitessier, N., Roggo, S., Veenstra, S., Tintelnot-Blomley, M., Rondeau, J.-M., Ostermeier, C., Strauss, A., Ramage, P., Paganetti, P., Neumann, U., and Betschart, C. (2005) Structure-based design, synthesis, and memapsin 2 (BACE) inhibitory activity of carbocyclic and heterocyclic peptidomimetics. *J. Med. Chem. 48*, 5175–5190.
10. Coburn, C. A., Stachel, S. J., Li, Y.-M., Rush, D. M., Steele, T. G., Chen-Dodson, E., Holloway, M. K., Xu, M., Huang, Q., Lai, M.-T., DiMuzio, J., Crouthamel, M.-C., Shi, X.-P., Sardana, V., Chen, Z., Munshi, S., Kuo, L., Makara, G. M., Annis, D. A., Tadikonda, P. K., Nash, H. M., Vacca, J. P., and Wang, T. (2004) Identification of a small molecule nonpeptide active site β-secretase inhibitor that displays nontraditional binding mode for aspartyl proteases. *J. Med. Chem. 47*, 6117–6119.
11. Jhoti, H., Cleasby, A., Verdonk, M., and Williams, G. (2007) Fragment-based screening using X-ray crystallography and NMR spectroscophy. *Curr. Opin. Chem. Biol. 11*, 485–493.
12. Murray, C. W., Callaghan, O., Chessari, G., Cleasby, A., Congreve, M., Frederickson, M., Hartshorn, M. J., McMenamin, R., Patel, S., and Wallis, N. (2007) Application of fragment screening by X-ray crystallography to β-secretase. *J. Med. Chem. 50*, 1116–1123.
13. Hong, L., Koelsch, G., Lin, X., Wu, S., Terzyan, S., Ghosh, A. K., Zhang, X. C., and Tang, J. (2000) Structure of the protease domain of memapsin 2 (β-secretase) complexed with inhibitor. *Science 290*, 150–153.

14. Huang, D., Lüthi, U., Kolb, P., Cecchini, M., Barberis, A., and Caflisch, A. (2006) In silico discovery of β-secretase inhibitors. *J. Am. Chem. Soc. 128*, 5436–5443.
15. Polgár, T., and Keserü, G. M. (2005) Virtual screening for β-secretase (BACE1) inhibitors reveals the importance of protonation states at Asp32 and Asp228. *J. Med. Chem. 48*, 3749–3755.
16. Park, H., and Lee, S. (2003) Determination of the active site protonation state of β-secretase from molecular dynamics simulation and docking experiment: implications for structure-based inhibitor design. *J. Am. Chem. Soc. 125*, 16416–16422.
17. Rajamani, R., and Reynolds, C. H. (2004) Modeling the protonation states of the catalytic aspartates in β-secretase. *J. Med. Chem. 47*, 5159–5166.
18. Yu, N., Hayik, S. A., Wang, B., Liao, N., Reynolds, C. H., and Merz, K. M., Jr (2006) Assigning the protonation states of key aspartates in β-secretase using QM/MM X-ray structure refinement. *J. Chem. Theory Comput. 2*, 1057–1069.
19. Spassov, V. Z., and Yan, L. (2008) A fast and accurate computational approach to protein ionization. *Protein Sci. 17*, 1955–1970.
20. Hong, L., Turner, R. T., III, Koelsch, G., Shin, D., Ghosh, A. K., and Tang, J. (2002) Crystal structure of mempasin 2 (β-secretase) in complex with an inhibitor OM00-3. *Biochemistry 41*, 10963–10967 Details of the synthesis of inhibitor OM00-3 are to be found in the Ph.D. Thesis of José Manuel Otero Casas (2007) Universidad de Santiago de Compostela (Spain).
21. Stachel, S. J., Coburn, C. A., Steele, T. G., Jones, K. G., Loutzenhiser, E. F., Gregro, A. R., Rajapakse, H. A., Lai, M.-T., Crouthamel, M.-C., Xu, M., Tugusheva, K., Lineberger, J. E., Pietrak, B. L., Espeseth, A. S., Shi, X.-P., Chen-Dodson, E., Holloway, M. K., Munshi, S., Simon, A. J., Kuo, L., and Vacca, J. P. (2004) Structure-based design of potent and selective cell-permeable inhibitors of human β-secretase (BACE-1). *J. Med. Chem. 47*, 6447–6450.
22. Rajapakse, H. A., Nantermet, P. G., Selnick, H. G., Munshi, S., McGaughey, G. B., Lindsley, S. R., Young, M. B., Lai, M.-T., Espeseth, A. S., Shi, X.-P., Colussi, D., Pietrak, B., Crouthamel, M.-C., Tugusheva, K., Huang, Q., Xu, M., Simon, A. J., Kuo, L., Hazuda, D. J., Graham, S., and Vacca, J. P. (2006) Discovery of oxadiazoyl tertiary carbinamine inhibitors of β-secretase (BACE-1). *J. Med. Chem. 49*, 7270–7273.
23. Charrier, N., Clarke, B., Cutler, L., Demont, E., Dingwall, C., Dunsdon, R., East, P., Hawkins, J., Howes, C., Hussain, I., Jeffrey, P., Maile, G., Matico, R., Mosley, J., Naylor, A., O'Brien, A., Redshaw, S., Rowland, P., Soleil, V., Smith, K. J., Sweitzer, S., Theobald, P., Vesey, D., Walter, D. S., and Wayne, G. (2008) Second generation of hidroxyethylamine BACE-1 inhibitors: optimizing potency and oral bioavailability. *J. Med. Chem. 51*, 3313–3317.
24. Ghosh, A. K., Kumaragurubaran, N., Hong, L., Kulkarni, S., Xu, X., Miller, H. B., Reddy, D. S., Weerasena, V., Turner, R., Chang, W., Koelsch, G., and Tang, J. (2008) Potent memapsin 2 (beta-secretase) inhibitors: design, synthesis, protein-ligand X-ray structure, and in vivo evaluation. *Bioorg. Med. Chem. Lett. 18*, 1031–1036.
25. Back, M., Nyhlén, J., Kvarnström, I., Appelgren, S., Borkakoti, N., Jansson, K., Lindberg, J., Nyström, S., Hallberg, A., Rosenquist, S., and Samuelsson, B. (2008) Design, synthesis and SAR of potent statine-based BACE-1 inhibitors: exploration of P1 phenoxy and benzyloxy residues. *Bioorg. Med. Chem. 16*, 9471–9486.
26. Citron, M., Oltersdorf, T., Haass, C., McConlogue, L., Hung, A. Y., Seubert, P., Vigo-Pelfrey, C., Lieberburg, I., and Selkoe, D. J. (1992) Mutation of the beta-amyloid precursor protein in familial Alzheimer's disease increases beta-protein production. *Nature 360*, 672–674.
27. Discovery Studio, version 2.1, Accelrys Inc., San Diego, CA.
28. Momany, F. A., Klimkowski, V. J., and Schäfer, L. (1990) On the use of conformationally dependent geometry trends from *ab initio* dipeptide studies to refine potentials for the empirical force field CHARMM. *J. Comput. Chem. 11*, 654–662.
29. Im, W., Lee, M. S., and Brooks, C. L., III (2003) Generalized Born model with a simple smoothing function. *J. Comput. Chem. 24*, 1691–1702.
30. Brooks, B. R., Bruccoleri, R. E., Olafson, B. D., States, D. J., Swaminathan, S., and Karplus, M. (1983) CHARMM: a program for macromolecular energy, minimization, and dynamics calculations. *J. Comput. Chem. 4*, 187–217.
31. Trylska, J., Antosiewicz, J., Geller, M., Hodge, C. N., Klabe, R. M., Head, M. S., and Gilson, M. K. (1999) Thermodynamic linkage between the binding of protons and inhibitors to HIV-1 protease. *Protein Sci. 8*, 180–195.
32. Piana, S., Sebastiani, D., Carloni, P., and Parrinello, M. (2001) Ab initio molecular dynamics-based assignment of the protonation state of pepstatin A/HIV-1 protease cleavage site. *J. Am. Chem. Soc. 123*, 8730–8737.
33. Coates, L., Tuan, H.-F., Tomanicek, S., Kovalevsky, A., Mustyakimov, M., Erskine, P., and Cooper, J. (2008) The catalytic mechanism of an aspartic protease explored with neutron and X-ray diffraction. *J. Am. Chem. Soc. 130*, 7235–7237.
34. Turner, R. T., III, Koelsch, G., Hong, L., Castanheira, P., Ghosh, A., and Tang, J. (2001) Subsite specificity of memapsin 2 (β-secretase): implications for inhibitor design. *Biochemistry 40*, 10001–10006.
35. Stachel, S. J., Coburn, C. A., Rush, D., Jones, K. L. G., Zhu, H., Rajapakse, H., Graham, S. L., Simon, A., Holloway, M. K., Allison, T. J., Munshi, S. K., Espeseth, A. S., Zuck, P., Colussi, D., Wolfe, A., Pietrak, B. L., Lai, M.-T., and Vacca, J. P. (2009) Discovery of aminoheterocycles as a novel β-secretase inhibitor class: pH dependence on binding activity part 1. *Bioorg. Med. Chem. Lett. 19*, 2977–2980.
36. Fornabaio, M., Cozzini, P., Mozzarelli, A., Abraham, D. J., and Kellogg, G. E. (2003) Simple, intuitive calculations of free energy of binding for protein-ligand complexes. 2. Computational titration and pH effects in molecular models of neuraminidase-inhibitor complexes. *J. Med. Chem. 46*, 4487–4500.